16th World Conference on Earthquake, 16WCEE 2017

Santiago Chile, January 9th to 13th 2017

Paper N° 3094

Registration Code: S-N1464752221

PERFORMANCE COMPARISON OF REGULAR AND SMART ELASTOMERIC ISOLATORS USING A NEW CONSTITUTIVE MODEL

F. Hedayati Dezfuli[(1)], S. Li[(2)], M. Shahria Alam[(3)]

[(1)] *Post Doctoral Fellow, University of British Columbia, farshad.hedayati@alumni.ubc.ca*
[(2)] *PhD Candidate, Southeast University of China, hmlishuai@163.com*
[(2)] *Associate Professor, University of British Columbia, shahira.alam@ubc.ca*

Abstract

Smart rubber bearings in which shape memory alloy (SMA) wires are incorporated possess improved performance compared to traditional steel- and fiber-reinforced elastomeric isolators. Recent studies discussed the feasibility of using such smart earthquake protective systems and showed that they have higher self-centering property and energy dissipation capacity. By proposing a novel smart isolation device, it is critical to properly establish a constitutive model which represents a relation between the input loading and the output response (hysteresis). Following this procedure is essential for properly evaluating characteristics of the smart isolation system and designing it. The objective of this study is to compare the seismic performance of regular and smart SMA-wire based rubber bearings using a new constitutive model developed by the same authors. This goal will be achieved by implementing the constitutive model in the finite element software, OpenSees. Results revealed that unlike the existing hysteresis model available for traditional rubber bearings, the new constitutive model, which has been developed for SMA wire-based isolators, can correctly simulate their hysteresis and capture their highly nonlinear shear response.

Keywords: *Shape Memory Alloy; Constitutive Model; Shear Hysteresis; Smart Elastomeric Isolator; Finite Element Simulation*

1. Introduction

Depending on the characteristics of elastomeric bearings (e.g. rubber, reinforcement, and supplementary elements), their shear hysteretic response is identified. By using different types of elastomer such as low-damping rubber [1, 2], commercial neoprene [3], and high damping rubber [4], different material models can be used. In numerical finite element method (FEM), as a reliable alternative for experimental approaches, low-damping rubber can be usually simulated using hyperelastic models because it follows the behavior of a hyperelastic material [5, 6]. Low damping elastomers have a low sensitivity to the loading history, temperature, and strain rate and as a result, are easy to model. However they possess insufficient energy dissipation capacity (2% - 3%). On the other hand, high-damping rubbers are expensive and show viscoelastic strain-rate-dependent behavior under shear deformations. So, the hyper-viscoelastic material model is a more appropriate choice for such elastomers [4, 7]. Lead rubber bearings (LRB) can provide a considerable amount of equivalent viscous damping ranging from 15% to 35% [8]. Main advantages of LRB are satisfactory amounts of rigidity, flexibility, and damping property at different load levels (e.g. service and earthquake) [8, 9]. A considerable amount of energy is dissipated when the lead yields and enters the plastic region. However, a major residual (unrecoverable) deformation occurs in the material after unloading.

Shape memory alloys (SMAs) with unique characteristics such as good energy dissipation capacity, re-centering capability (up to 13.5% superelastic strain in iron-based alloy, FeNiCoAlTaB) [10] and fatigue property [11-13] are excellent candidates to be employed as supplementary elements in elastomeric bearings (EBs). Smart base isolators in which SMA is used in various forms (e.g. wire, bar, or spring) are introduced as new generations of base isolation systems with an improved performance. It is highly beneficial to implement SMAs in EBs in order to extend their service life by improving their self-centering and damping properties. These improvements are achieved by increasing the shear deformation capacity, controlling the displacement and limiting the force transmitted to the superstructure. In a feasibility study, Attanasi et al. proposed an innovative SMA-based isolation device and showed that although there is a big difference in the hysteretic responses of SMA device (flag-shaped hysteresis model) and LRB (elasto-plastic model), both systems have similar displacement and force demands [14]. However, the main advantage of SMA-based device over LRB was zero residual deformation. They concluded that using SMA as a lateral restrainer can improve the re-centering property and energy dissipation capacity of bearing systems. Choi et al. proposed an SMA wire-based rubber bearing (SMA-RB) for highway steel bridges and compared its performance with that of a LRB [15]. They showed that SMA wires can satisfactorily restrain the superstructure from over-displacement. In a numerical work conducted by [16], SMA wires were implemented into a high damping rubber bearing (HDRB) with a cross configuration. In order to identify the efficiency of the SMA-HDRB, they evaluated the seismic response of a three-span continuous steel-girder RC-pier supported bridge, which was isolated by the proposed SMA-HDRB. They modeled the hysteretic behavior of the smart isolator using a bilinear kinematic hardening (BKH) model. Although they considered different mechanical properties (e.g. initial stiffness and post-yield hardening ratio), insignificant differences were observed in the performances. The reason was due to the BKH model which was not able to correctly simulate the actual response of SMA-HDRB.

This research aims to accurately model the shear hysteretic behavior of SMA-wire based rubber bearings and assess the seismic response of a bridge structure isolated by such smart bearings. In this regard, the constitutive model of SMA-LRB, which has been developed by [17], is implemented into the finite element software OpenSees [18] and then, the dynamic response of the smart isolator is simulated. It should be noted that there is no finite element-based software product equipped with such a constitutive model. The structure is a three-span continuous steel girder bridge isolated, in two different cases, using regular and smart elastomeric bearings. Three responses including relative displacement and energy dissipation capacity of bearings; and base shear of bridge piers are evaluated.

2. SMA Wire-based LRB

A new generation of smart elastomeric isolators, called SMA-LRB, is designed with a constitutive model proposed by [17]. As shown in Fig. 1, the isolation system includes two parts: a lead rubber bearing and a double cross configuration of SMA wires (i.e. DC-SMAW). Since on each side of the LRB, two crosses are formed due to passing continuous SMA wires 1 and 2 through hooks (located at specified spots), the configuration of SMA wires is called double cross. Physical properties of LRB and iron-based SMA wires (FeNiCoAlTaB) are listed in Table 1.

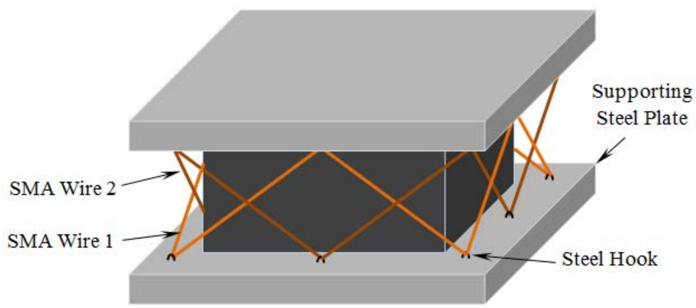

Fig. 1 – Lead Rubber bearing equipped with double cross SMA wires (SMA-LRB)

Table 1 –Properties of LRB and SMA wire

LRB		**Ferrous SMA wire**	
Length (mm)	350	Cross sectional radius, r_{SMA} (mm)	2.7
Width (mm)	350	Elastic modulus at austenite, E^A (GPa)	46.9
Height (mm)	102	Austenite finish temperature, A_f (°C)	-62.0
Number of rubber layers	13	Superelastic strain limit	13.5%
Thickness of rubber layers (mm)	6		
Thickness of reinforcement (mm)	2		
Diameter of lead core (mm)	80		

In the model, the behavior of LRB was idealized using the bilinear kinematic hardening model characterized by three distinct features: initial stiffness K_0, yield force F_y and post-yield hardening ratio r. A hysteresis model characterized by three stiffnesses for DC-SMAW was developed: $K_{0,w}$, K_i, and K_r are the initial stiffness, the intermediate stiffness, and the re-centering stiffness, respectively. In this study, the proposed constitutive model of SMA-LRBs is implemented in OpenSees [18] as two new User Elements for LRB and DC-SMAW. Here, LRB and DC-SMAW used by [19] are chosen as the reference and the mechanical properties of LRB, which is idealized as a bilinear model, as well as the DC-SMAW model are given in Table 2.

Table 2 – Mechanical properties of the LRB and DC-SMA wire

LRB bilinear model		**DC-SMAW model**	
Initial stiffness K_0 (kN/mm)	14.8	Initial stiffness, $K_{0,w}$ (kN/mm)	0.94
Yield force F_y (kN)	37.8	Intermediate stiffness K_c (kN/mm)	3.23
Post-yielding hardening ratio r	0.05	Re-centering stiffness K_r (kN/mm)	0.44

To ensure that the new elements are working properly in any condition, the results, which are attained from OpenSees, are compared with those obtained from MATLAB [20] code for different functions such as ramp, step, sinusoidal, and a combination of them with different peak amplitudes and strain rates. Three excitations (E1, E2 and E3) are chosen as the input displacements and plotted in Fig. 2.

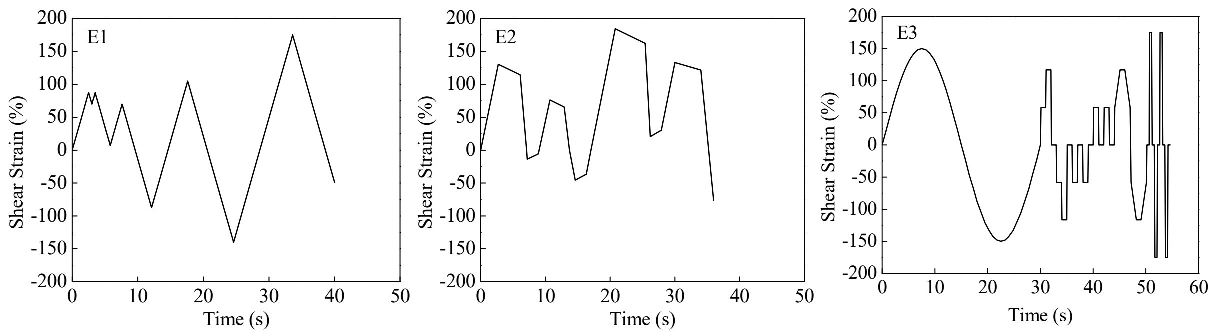

Fig. 2 – Normalized input displacement

Fig. 3 shows responses of the DC-SMAW and LRB obtained from OpenSees and MATLAB. The comparison shows a good agreement between the two approaches, which reveals that the new elements developed in OpenSees is capable of accurately predicting the re-centering capability and energy dissipation capacity of SMA-LRB under different excitations.

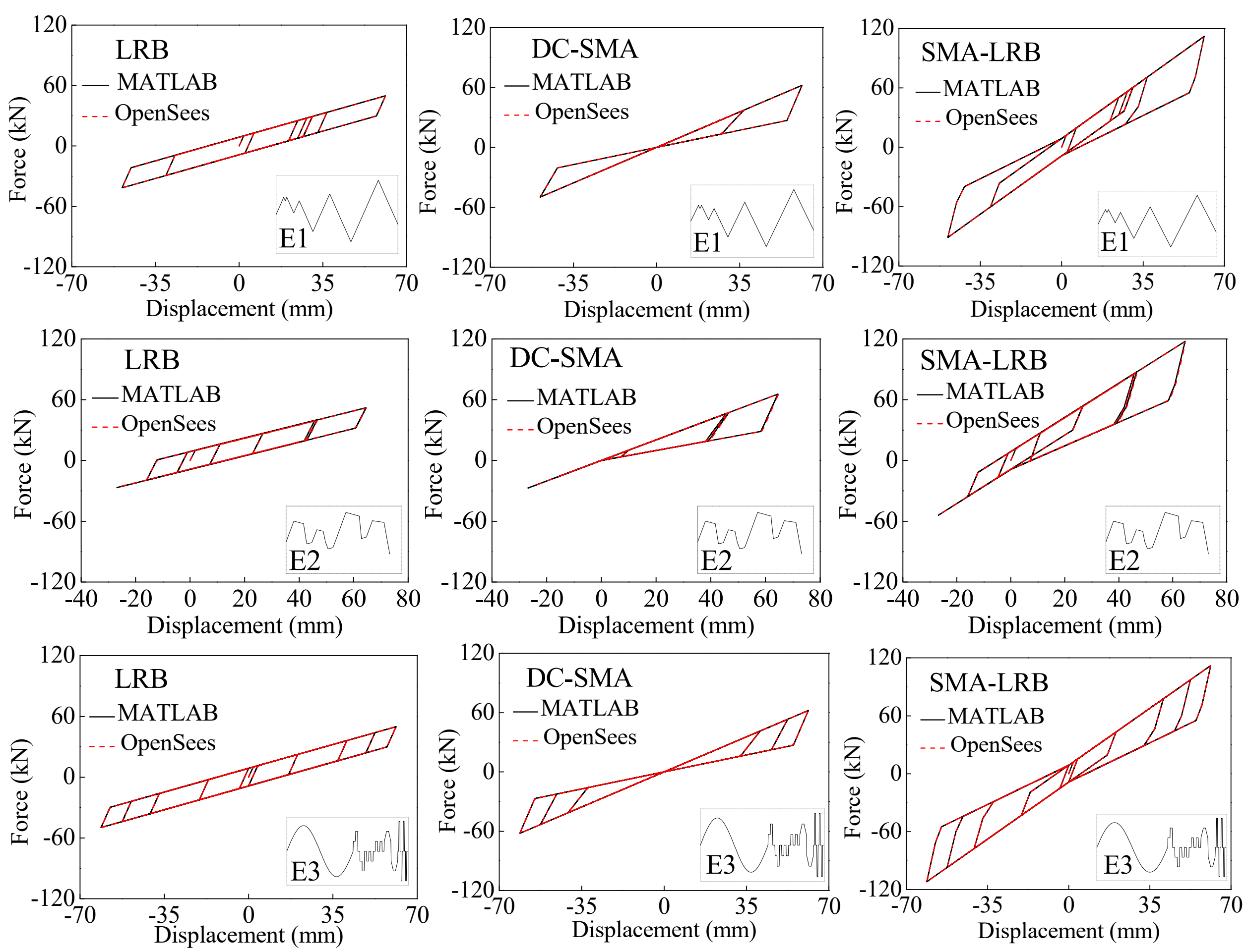

Fig. 3 – Responses of LRB and DC-SMA obtained from OpenSees and MATLAB

3. Seismic Response of a Steel-Girder Bridge

In order to investigate the seismic performance of the SMA-based LRBs, a three-span continuous steel girder reinforced-concrete (RC) pier supported bridge is modeled and analyzed under seismic ground motions using OpenSees. In this regard, time history analyses are performed for three earthquake records, as listed in Table 3. Considering PGA as the intensity measurement, the PGA values of the selected records are larger than 0.2g with epi-central distances higher than 10 km. The bridge (shown in Fig. 4) with a skew angle of 20° consists of a continuous RC deck-steel girder which is isolated by 6 rubber bearings installed between the steel girder and pier caps. The detailed dimensions of each component are available in [19].

The steel girders and pier caps are modeled with elastic beam-column elements so that they remain elastic under earthquake excitation. Girders are divided into a number of small discrete segments. To represent the distribution of the material nonlinearity along the length of piers, the fiber-modeling approach is implemented. Each fiber section consists of the unconfined concrete, the confined concrete and the longitudinal steel reinforcement. Chang and Mander (1994) uniaxial steel model simulates the behavior of the reinforcements and the Kent-Park constitutive relationship is used to model the nonlinear behavior of the concrete. The effect of abutment and the soil-structure interaction are not considered in this study.

In order to assess the performance of LRBs and SMA-LRBs, the seismic response of the bridge equipped with these rubber bearings is evaluated and compared to that of the non-isolated bridge. LRBs and SMA-LRBs are modeled by using the new elements developed and implemented in OpenSees by the authors.

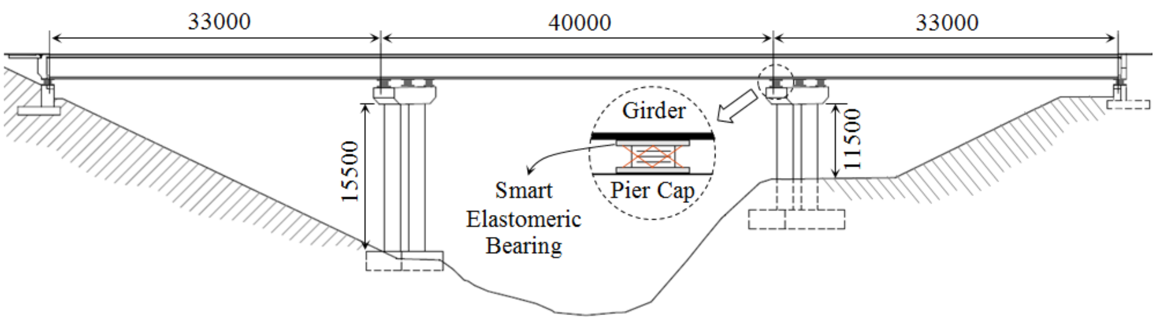

Fig. 4 – Multi-span continuous steel girder bridge (dimensions are in mm)

Table 3 – Description of the ground motions used in the analysis

Earthquake	Magnitude	R_{rup} (km)	Station, component	PGA (g)	PGV (cm/s)
Imperial Valley 1979	6.5	10.5	CXO225	0.27	22.5
Coalinga 1983	6.4	24.0	CAK360	0.28	25.8
Landers 1992	7.3	19.74	CLW-TR	0.42	42.3

4. Results and Discussion

In order to compare performances of regular and smart rubber bearings considered in this study (i.e. LRB and SMA-LRB), relative displacement and energy dissipation capacity of isolation systems as well as shear force at the pier support are calculated and results are presented.

4.1 Lateral displacement and hysteretic behavior of bearings

Variations of shear strain (i.e. normalized lateral displacement) in LRB and SMA-LRB over the time during which earthquakes happen are plotted in Fig. 5. To quantitatively compare the results, the peak shear strain, γ_{max}, of LRB and SMA-LRB are listed in Table 4 for three ground motions. Under Imperial Valley 1979, Coalinga 1983 and Landers 1992 earthquakes, the maximum shear strain of SMA-LRBs decreases by 47%, 33% and 19% compared to that of LRBs, respectively. SMA-LRBs can efficiently prevent instability of the bearings and unseating of the bridge deck. Additionally, LRBs retain residual deformation under Coalinga and Landers earthquakes. However, the SMA-LRBs recover the original form at the end of earthquakes.

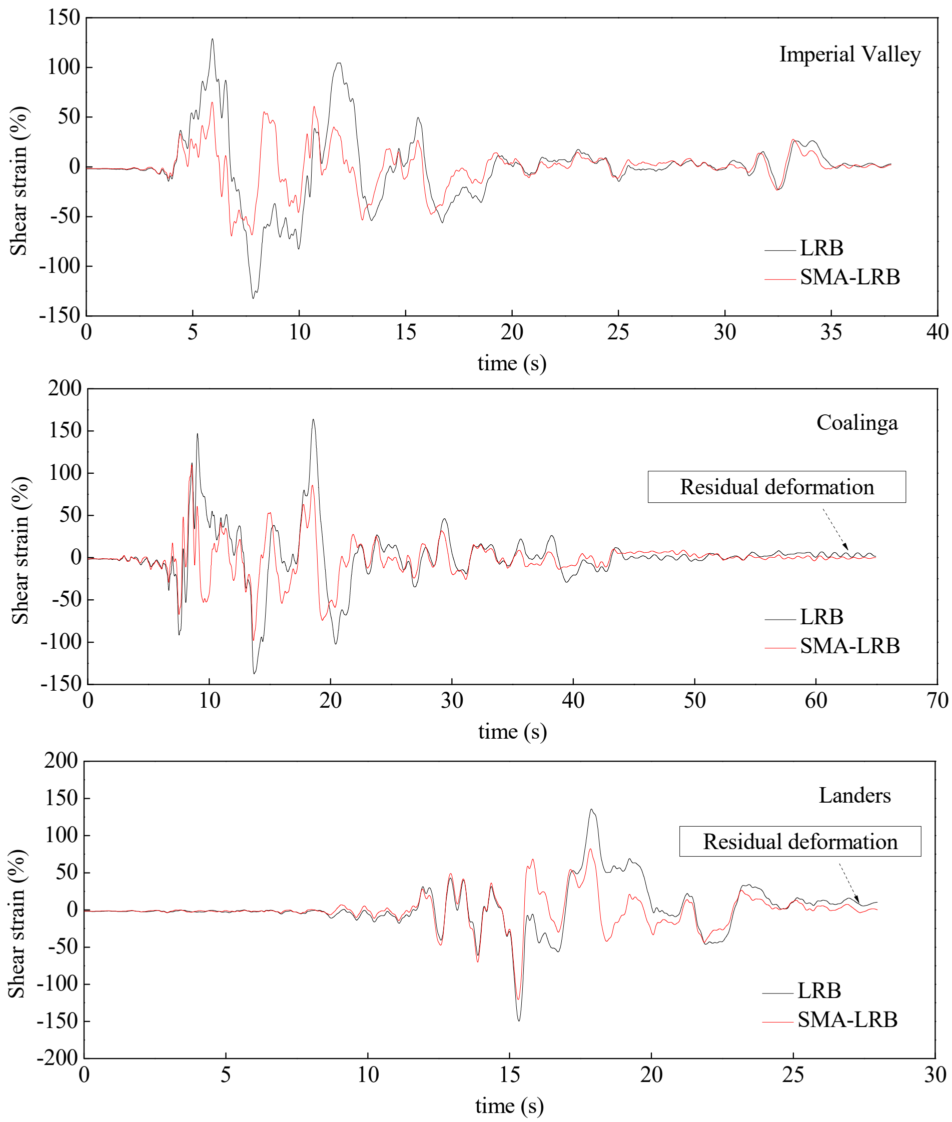

Fig. 5 – Time history of shear strain in LRB and SMA-LRB excited by three earthquake records

Table 4 – Peak shear strain of rubber bearings under different earthquake records

Rubber bearing	**Imperial Valley**		**Coalinga**		**Landers**	
	γ_{max} (%)	Δ	γ_{max} (%)	Δ	γ_{max} (%)	Δ
LRB	132		164		150	
SMA-LRB	70	-47%	110	-33%	121	-19%

Hysteretic response of LRB and SMA-LRB excited by three considered earthquakes are depicted in Fig. 6. As can be observed, SMA-LRB transfers a higher amount of shear force to the superstructure due to a higher stiffness. In fact, double cross SMA wires increases the lateral effective stiffness of the isolation system. The reason is that when the top supporting plate of the LRB is laterally displaced, SMA wires are elongated and as a result, a tensile force is generated in each wire. This force (i.e. the resultant force) is transferred to the LRB in the opposite direction of the movement. Therefore, the flexibility of the whole system (SMA-LRB) decreases and the horizontal stiffness increases. Due to the decrease of the lateral displacement, the total dissipated energy of SMA-LRBs, which is the area inside the force-displacement curves, may be smaller or higher than that of LRBs under a certain earthquake excitation. However, if the maximum lateral displacement is the same for SMA-LRB and LRB, the dissipated energy of the smart isolator is significantly higher than that of the regular one (LRB). This fact reveals that SMA-LRB has a superior damping property. According to the results listed in Table 5, the capability of SMA-LRB in dissipating the energy is 2% and 17% higher than that of LRB under Coalinga and Landers earthquakes, respectively, whereas, 4% smaller under Imperial Valley earthquake.

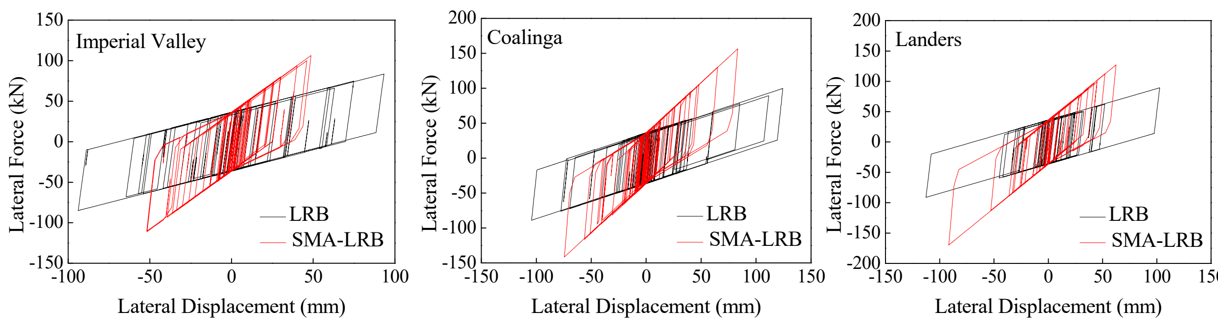

Fig. 6 – Hysteretic behavior of LRB and SMA-LRB under three earthquake records

Table 5 – Total energy dissipated by LRB and SMA-LRB under different earthquake records

Rubber bearing	**Imperial Valley**		**Coalinga**		**Landers**	
	U_D (kJ)	Δ	U_D (kJ)	Δ	U_D (kJ)	Δ
LRB	41.5		63.0		38.0	
SMA-LRB	39.8	-4%	64.3	2%	44.3	17%

4.2 Pier Response

Fig. 7 shows the time history of the shear force generated at the base of piers (i.e. structural base shear) due to seismic excitations for non-isolated bridge, and bridges isolated by LRB and SMA-LRB. The peak base shears are also listed in Table 6. Compared to non-isolated bridge, when the structure is isolated by LRB, the maximum base shear reduces by 30%, 13%, and 43% for Imperial Valley, Coalinga and Landers earthquakes, respectively. Using SMA wires in LRB can improve the seismic response of the isolated bridge in terms of base shear reduction. Although peak base shears in cases of LRB and SMA-LRB are very close to each other under three ground motions; using SMA-LRB as the isolator could reduce the maximum base shear by 31% and 15% for Imperial Valley and Coalinga records, respectively, compared to non-isolated bridge.

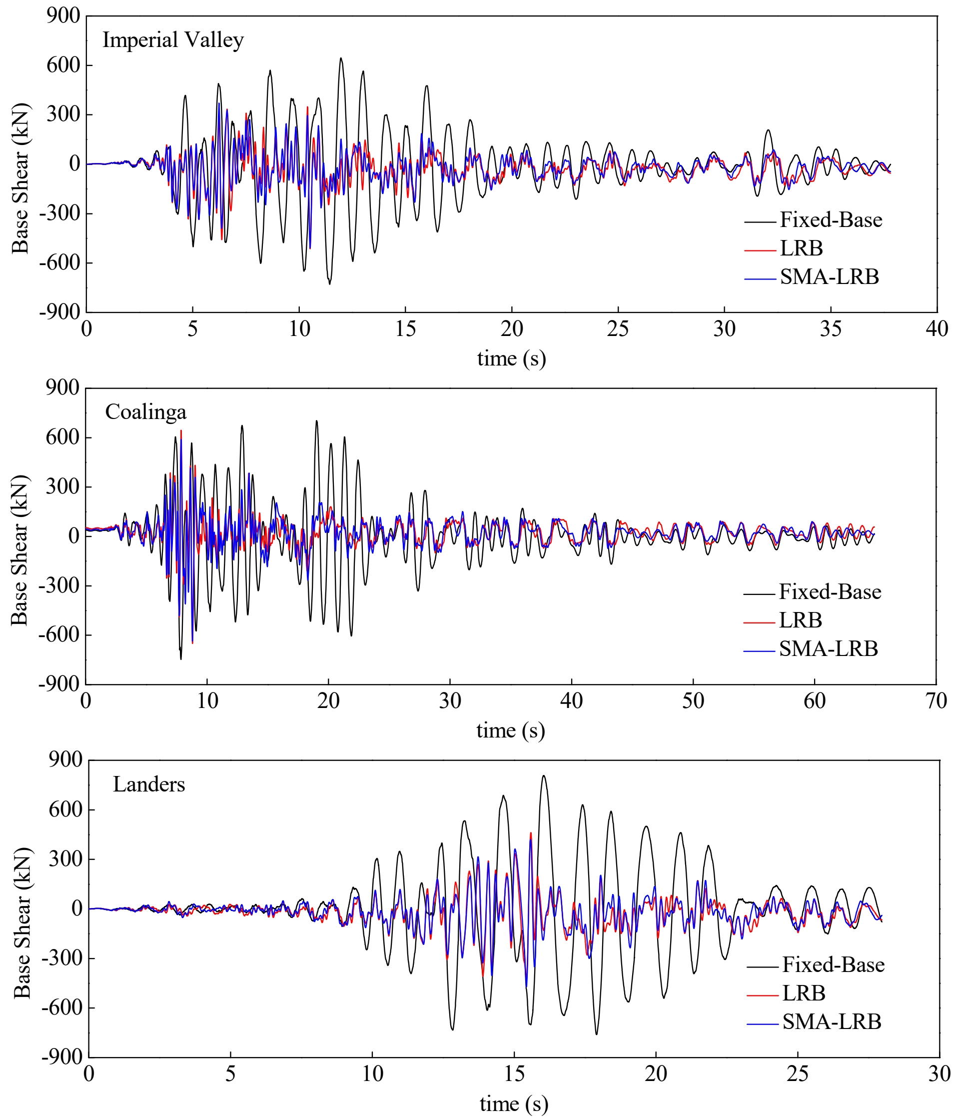

Fig. 7 – Time history of the base shear in the piers under three earthquake records

Table 6 – Peak base shear in the non-isolated and isolated bridges under three earthquake records

Bridge isolated by	**Imperial Valley**		**Coalinga**		**Landers**	
	F_{max} (kN)	Δ	F_{max} (kN)	Δ	F_{max} (kN)	Δ
Non	729		747		808	
LRB	513	-30%	650	-13%	462	-43%
SMA-LRB	505	-31%	636	-15%	470	-42%

5. Conclusion

A newly developed constitutive model of SMA-wire based rubber bearings was implemented in OpenSees and the seismic response of a bridge structure equipped with such SMA-LRBs was investigated. In the proposed hysteresis model of SMA-LRB, a kinematic bilinear model for LRB was combined with a new model for DC-SMA wires, which is characterized by three stiffnesses (i.e. initial, intermediate, and re-centering).

Comparing the shear hysteretic responses of SMA-LRBs obtained from OpenSees and Matlab codes under different excitations, showed that this FE-based software (OpenSees) is capable of correctly capturing the nonlinear behavior of the SMA-LRB.

Using double cross SMA wires made of iron-based alloys (FeNiCoAlTaB) with around 13.5% superelastic strain limit reduced the shear strain demand in SMA-LRBs by increasing the effective stiffness of elastomeric isolator. Another finding was that the flag-shaped hysteresis of SMA with zero residual deformation could enhance the re-centering property and increase the energy dissipation capacity of lead rubber bearing. SMA wires not only could improve the mechanical response of elastomeric isolators, but also could reduce the shear force at the base of the piers by decreasing the acceleration of the bridge deck.

A comprehensive parametric study should be conducted to investigate the effect of geometry and mechanical properties of SMA wires and SMA-RBs (e.g. radius of wires and stiffness of rubber bearing) on the seismic response of bridge components (e.g. residual deformation of bearing, acceleration of deck, bending moment of piers).

6. References

[1] Amin AFMS, Alam MS, Okui Y (2002): An improved hyperelasticity relation in modeling viscoelasticity response of natural and high damping rubbers in compression: experiments, parameter identification and numerical verification. *Mechanics of Matererials* 34(2): 75-95.

[2] Gjorgjiev I, Garevski M (2013): A polynomial analytical model of rubber bearings based on series of tests. *Engineering Structures*, 56: 600-609.

[3] Hedayati Dezfuli F, Alam MS (2013). Sensitivity analysis of carbon fiber-reinforced elastomeric isolators based on experimental tests and finite element simulation. *Bulletin of Earthquake Engineering*, doi: 10.1007/s10518-013-9556-y.

[4] Hedayati Dezfuli F, Alam MS (2012): Material modeling of high damping rubber in finite element method. *3rd International Structural Specialty Conference*, June 6-9, 2012. Edmonton, Alberta, Canada.

[5] Hossa L, Marczak RJ (2010): A new constitutive model for rubber-like materials. Mecánica Computacional. Vol. XXIX: 2759-2773.

[6] Ali A, Hosseini M, Sahari BB (2010): A Review of constitutive models for rubber-like materials. *American Journal of Engineering and Applied Sciences*, 3(1): 232-239.

[7] Bergstrom JS, Boyce MC (1998): Constitutive modeling of the large strain time-dependent behavior of elastomers. *Journal of the Mechanics and Physics of Solids*, 46(5): 931-954.

[8] Kelly TE (2001): Base isolation of structures- design guidelines. Holmes Consulting Group Ltd, Wellington, New Zealand.

[9] Chen L, Jiang L, Liu P (2011): Dynamic properties of lead rubber bearings and its seismic isolation applications in high-speed railway bridge. *Advanced Materials Research*, 150-151: 164-167. doi: 10.4028/www.scientific.net/AMR.150-151.164.

[10] Tanaka Y, Himuro Y, Kainuma R, Sutou Y, Omori T, Ishida K (2010): Ferrous polycrystalline shape-memory alloy showing huge superelasticity. Science, 327(5972): 1488-1490.

[11] Eggeler G, Hornbogen E, Yawny A, Heckmann A, Wagner M (2004): Structural and functional fatigue of NiTi shape memory alloys, *Materials Science and Engineering: A*; 378(1-2): 24-33.

[12] Hornbogen E (2004): Review: Thermo-mechanical fatigue of shape memory alloys, *Journal of Materials Science*; 39(2): 385-399.

[13] Alam MS, Youssef MA, Nehdi M (2007): Utilizing shape memory alloys to enhance the performance and safety of civil infrastructure: A review. *Canadian Journal of Civil Engineering*, 34: 1075-1086.

[14] Attanasi G, Auricchio F, Fenves GL (2009): Feasibility assessment of an innovative isolation bearing system with shape memory alloys. *Journal of Earthquake Engineering*, 13:18-39. doi:10.1080/13632460902813216.

[15] Choi E, Nam TH, Cho BS (2005): A new concept of isolation bearings for highway steel bridges using shape memory alloys. *Canadian Journal of Civil Engineering,* 32(5): 957-967.

[16] Hedayati Dezfuli F, Alam MS (2014): Performance-based assessment and design of FRP-based high damping rubber bearing incorporated with shape memory alloy wires. *Engineering Structures*, 61 (2014) 166-183.

[17] Hedayati Dezfuli F, Alam MS (2015): Hysteresis model of shape memory alloy wire-based laminated rubber bearing under compression and unidirectional shear loadings. *Smart Materials and Structures*, 24 065022.

[18] McKenna F, Fenves GL, Scott MH (2000): Open system for earthquake engineering simulation (OpenSees). Berkeley, CA: University of California. Available from http://opensees.berkeley.edu.

[19] Hedayati Dezfuli F, Alam MS (2016): Effect of different steel-reinforced elastomeric isolators on the seismic fragility of a highway bridge. *Structural Control and Health Monitoring*, doi: 10.1002/stc.1866.

[20] The MathWorks, Inc. MATLAB R2012b, Version 8, 2012.